

Noise Resilience Benchmarking of Hybrid Quantum-Classical Face Verification Under NISQ Constraints

Jacky Jiang¹, Xinning Wang²

¹Department of Electrical and Computer Engineering, University of Waterloo, Waterloo, Ontario N2L 3G1, Canada

²Institute for Quantum Computing, University of Waterloo, Waterloo, Ontario N2L 3G1, Canada

Hybrid quantum-classical neural networks have emerged as a promising paradigm for Noisy Intermediate-Scale Quantum (NISQ) devices, where small variational quantum circuits (VQCs) can be combined with powerful classical backbones. In this project, we use an end-to-end face verification pipeline that detects, aligns, and embeds facial images using a pretrained ResNet-18 encoder, and then attaches three alternative readout heads: (i) a conventional classical fully connected classifier, (ii) a hybrid model in which a learnable four-dimensional feature projection is processed by a four-qubit VQC, and (iii) a “diverse vote” ensemble composed of several independently trained hybrid experts. We evaluate these models on a held-out verification dataset and observe that hybrid and ensemble architectures not only match but often outperform the classical baseline in the noise-free setting, while also exhibiting reduced sensitivity to initialization. To assess their suitability for near-term quantum hardware, we further inject three physically motivated noise channels—amplitude damping, phase damping, and coherent over-rotation—into the VQC during inference. The resulting degradation patterns provide a quantitative characterization of noise resilience for hybrid architectures on a realistic computer-vision task. Overall, our study illustrates how small VQCs can be effectively integrated into classical vision pipelines and highlights the potential of ensemble-based hybrid models as a stabilizing mechanism for NISQ-era applications.

Index Terms—Quantum machine learning, variational quantum circuits, hybrid quantum-classical networks, NISQ, face verification.

I. INTRODUCTION

THE current generation of quantum devices—the Noisy Intermediate-Scale Quantum (NISQ) era—offers processors with tens to a few hundred qubits, but limited coherence times and imperfect gate operations strongly restrict circuit depth and algorithmic reliability. As fully quantum, fault-tolerant algorithms remain out of reach, a practical alternative is to embed small variational quantum circuits (VQCs) inside largely classical pipelines. This hybrid approach has been explored broadly in quantum machine learning (QML), where parametrized quantum circuits act as learnable nonlinear modules within otherwise classical architectures [1], [3].

Variational circuits are often proposed as expressive feature maps that may leverage entanglement or high-dimensional Hilbert space structure. However, their performance is tightly linked to trainability, circuit expressivity, and vulnerability to hardware noise. A growing body of work has therefore examined how amplitude damping, phase damping, depolarizing channels, and biased noise processes distort variational models and their gradients [4], [5], [6]. Yet these studies typically analyze circuits in isolation rather than in the context of realistic end-to-end applications.

Face verification provides a compelling setting to study hybrid models. Modern systems use deep convolutional networks (CNNs) to align faces and extract compact embeddings—often via residual architectures such as ResNet-18 or ResNet-50—after which verification reduces to comparing embeddings in latent space. Prior work has explored hybrid quantum-classical convolutional networks [7], [8], and several recent studies apply quantum components to face recognition or related tasks [10]. However, most results focus on single-model performance under idealized, noise-free conditions, leaving

open questions about robustness, variance across training runs, and whether classical ensemble techniques can stabilize hybrid quantum heads.

These gaps are further underscored by the lack of task-level benchmarks that evaluate how standard quantum noise channels affect downstream metrics such as classification accuracy. While circuit-level noise resilience is well studied, relatively little is known about how noise propagates through a hybrid architecture built on top of a strong classical backbone, or whether quantum components retain any advantage when subjected to realistic NISQ-style noise.

In this work, we address these questions through a concrete case study on binary face verification. Using a pretrained ResNet-18 to generate 512-dimensional embeddings, we compare three readout strategies: (i) a purely classical fully connected head, (ii) a single hybrid head that compresses the embedding to four features and processes them with a four-qubit VQC, and (iii) a “diverse vote” ensemble consisting of several independently trained hybrid experts that share the classical backbone. This design aligns with NISQ restrictions, where executing multiple shallow circuits in parallel is more feasible than building a single deep quantum network.

To probe noise resilience, we inject amplitude-damping (T_1 -like), phase-damping (T_2 -like), and coherent over-rotation noise directly into the quantum circuit during inference. We then quantify how each noise type affects accuracy for both single-hybrid and ensemble models.

The primary contributions of this paper are:

- constructing an end-to-end hybrid quantum-classical pipeline for face verification and benchmarking it against a strong classical baseline;
- demonstrating that small hybrid ensembles improve stability and variance reduction relative to single VQCs;

- providing one of the first application-level evaluations of how standard quantum noise channels affect hybrid model performance on a realistic vision task.

The remainder of the paper presents related background (Section II), our system design and noise-injection framework (Section III), experimental results (Section IV), and a discussion of limitations and future directions (Section V).

II. METHODOLOGY

A. Task Formulation and Dataset

We cast face verification into a binary image-classification task. Each aligned face crop is assigned a label $y \in \{0, 1\}$, where $y = 1$ denotes a genuine (positive) example and $y = 0$ denotes an impostor (negative) example. Although verification is naturally a pairwise problem, training at the single-image level is standard in feature-learning pipelines: the CNN backbone learns a discriminative embedding, and pairwise verification can later be performed by comparing embeddings or combining classifier scores. This formulation allows the quantum head to operate on a compact feature vector rather than on raw pixel pairs, enabling simpler training dynamics while still supporting verification-style evaluation at test time.

Our dataset is constructed from a public face collection together with a small self-collected set of additional positive examples. After basic quality filtering and face detection, we obtain 600 labeled face images (300 positive and 300 negative) for training and validation. We use an 80/20 train-validation split (480/120 images) and reserve a disjoint test set of 340 images. All experiments reported in this paper use the same fixed split.

B. Preprocessing Pipeline

We use a two-stage preprocessing pipeline: an offline alignment stage that prepares 224×224 face crops, followed by online normalization and augmentation at training time.

a) Offline face detection and alignment: We run an MTCNN-based detector and aligner (from facenet_pytorch) over all RGB images in the raw dataset using a standalone script. The detector is configured with:

- output size 224×224 pixels,
- a margin of 20 pixels around the detected bounding box,
- a minimum face size of 40 pixels.

For each input image, MTCNN returns either a single aligned face crop or a stack of multiple faces. In the default setting we keep only the best face per image, which corresponds to the highest-confidence detection. The crop is converted back to an RGB image and saved as a JPEG file under an output root directory that mirrors the original directory structure. Thus, class labels (e.g., positive vs. negative) are inherited directly from the folder names. Images in which no face is detected are discarded.

b) Online normalization and DataLoader: Downstream models operate on the aligned crops. We build PyTorch dataloaders on top of the aligned directory using `torchvision.datasets.ImageFolder`. Each 224×224 RGB face is converted to a tensor and normalized channel-wise with standard ImageNet statistics:

$$\mu = [0.485, 0.456, 0.406], \quad \sigma = [0.229, 0.224, 0.225].$$

For the classical and hybrid models we apply light data augmentation on the training set (random horizontal flips and mild color jitter), while the validation and test sets use only the deterministic normalization transform. This ensures that all models see a consistent, standardized input representation.

C. Classical ResNet-18 Baseline

As a baseline we fine-tune a ResNet-18 model initialized with ImageNet weights. The final fully connected (FC) layer is replaced by a small binary classification head. For the two-class setting we use a single logit and a sigmoid output, equivalent to a two-logit softmax up to a constant shift.

The model is trained in two phases. First, we freeze all convolutional layers and train only the new FC head for a few epochs, allowing it to adapt to the new domain. Second, we unfreeze the backbone and fine-tune the entire network with a smaller learning rate on the earlier layers. Training uses an AdamW optimizer with a cosine-annealing learning-rate schedule, label smoothing, and a class-weighted loss to compensate for any slight imbalance between positive and negative examples. Early stopping on validation accuracy is used to select the final checkpoint.

On the held-out test set, this classical baseline achieves an accuracy of 90.29% (307/340 images), which serves as the reference point for evaluating our hybrid variants.

D. Hybrid Quantum Head

To incorporate a quantum component into the classification pipeline, we replace the classical fully connected (FC) head with a variational quantum circuit (VQC) while keeping the ResNet-18 backbone frozen during hybrid training. The hybrid head follows an “encode–transform–measure” structure that maps the 512-dimensional ResNet embedding into quantum expectation values suitable for downstream classification.

a) Learned projection $L_{512 \rightarrow 4}$: The 512-dimensional embedding h produced by the ResNet backbone is first mapped to a four-dimensional feature vector

$$x = L_{512 \rightarrow 4}(h),$$

followed by a tanh activation so that $x \in [-1, 1]^4$. Each component x_i represents a task-adapted latent coordinate that will be encoded as a rotation angle on qubit i . All parameters of this projection layer are learned jointly with the VQC parameters.

b) *Quantum encoding and variational circuit.*: We employ a 4-qubit quantum circuit with angle encoding. Each feature x_i initializes qubit i through the sequence

$$|0\rangle \xrightarrow{H R_Y(\theta_i)} |\phi_i\rangle, \quad \theta_i = \frac{\pi}{2} x_i.$$

This encoding step is followed immediately by a noise channel when operating in the noisy setting.

The encoded state then passes through a hardware-efficient variational ansatz consisting of six identical layers. Each layer contains:

- four trainable single-qubit rotations $R_Y(w_i^{(l)})$ (one per qubit), and
- a fixed ladder-pattern entangling block composed of three CNOT gates acting on qubit pairs $(1, 2)$, $(0, 1)$, and $(2, 3)$.

Each layer thus contributes four trainable parameters, yielding a total of $6 \times 4 = 24$ VQC parameters.

In the noisy configuration (`default.mixed`), we insert amplitude-damping, phase-damping, or coherent over-rotation channels after the encoding step and after each single-qubit rotation inside every variational layer. This placement follows a gate-level noise model and captures the cumulative effect of decoherence and systematic miscalibration.

c) *Measurement and classical readout $L_{4 \rightarrow 2}$.*: At the output of the circuit, we measure the expectation value of the Pauli-Z operator on all four qubits. This vector is fed into a final linear readout $L_{4 \rightarrow 2}$ which produces logits for binary classification. During hybrid training, gradients flow through the projection layer, all VQC parameters, and the final classifier, while the ResNet backbone is evaluated under `torch.no_grad()`.

The complete hybrid quantum head—including the encoding stage and all six variational layers—is shown in Fig. 1.

E. Diverse Hybrid Ensemble

While a single 4-qubit, depth-6 VQC is expressive, it can exhibit significant variability across random seeds due to the highly nonconvex optimization landscape. To mitigate this variance and improve robustness, we construct an ensemble of $K = 5$ hybrid experts that share the same classical backbone but differ in their quantum components.

All experts use:

- the same frozen ResNet-18 backbone, and
- identical training, validation, and test splits.

Diversity among experts is introduced through three mechanisms:

- **Bootstrap sampling of embeddings.** Backbone outputs for all training images are first cached. Each expert is then trained on a bootstrap sample (with replacement) of these embeddings, providing classical bagging at the feature level.
- **Distinct circuit structures.** Although all experts use 4 qubits and 6 variational layers, they differ in their entangling topology. In addition to the nearest-neighbor ladder pattern shown in Fig. 1, ensemble members are assigned alternative layouts such as ring-style couplings and *randomly chosen two-qubit connections*. These random couplings may include non-nearest-neighbor CNOTs—i.e.,

CNOT gates between qubits that are not adjacent in the baseline circuit—yielding entanglement graphs with different connectivity profiles and inducing meaningfully different quantum decision boundaries.

- **Independent parameter initialization.** The projection layer, the 24 VQC parameters, and the final linear readout are initialized independently for each expert, further diversifying model behavior.

At inference time, each expert produces logits $(z_0^{(k)}, z_1^{(k)})$. We calibrate expert outputs using temperature scaling on the validation set, then aggregate predictions via soft voting across calibrated logits or probabilities. Because all experts share the same frozen backbone features, this ensemble strategy incurs minimal runtime overhead while providing substantially improved stability relative to any single hybrid model.

These three diversity mechanisms—bootstrap sampling, heterogeneous entangling structures, and independent initialization—were selected to ensure that experts explore genuinely different regions of the variational landscape. Preliminary experiments showed that ensembles relying only on initialization diversity provided limited benefit, whereas introducing structural diversity—particularly through non-nearest-neighbor entangling patterns—significantly reduced variance across runs. This suggests that, for shallow VQCs, topological diversity may be as important as data diversity for stabilizing hybrid models.

F. Noise Models and Quantum Simulation

To assess the behavior of the hybrid quantum head under realistic NISQ conditions, we inject several standard noise channels into the quantum circuit. These channels are parameterized by the characteristic coherence times T_1 and T_2 of a qubit, which quantify energy relaxation and dephasing, respectively [12].

- **T_1 (energy-relaxation time).** Governs incoherent decay from $|1\rangle$ to $|0\rangle$ due to coupling with the environment.
- **T_2 (dephasing time).** Characterizes loss of phase coherence between $|0\rangle$ and $|1\rangle$ without changing their populations.

In a gate-based simulation, these continuous-time processes are converted into *per-gate* noise parameters using the standard exponential relation

$$\gamma_1 = 1 - e^{-t_{\text{gate}}/T_1}, \quad \gamma_2 = 1 - e^{-t_{\text{gate}}/T_2},$$

where t_{gate} denotes the effective duration assigned to one variational layer. Instead of specifying physical times in nanoseconds, we normalize $t_{\text{gate}} = 1$ unit and choose T_1 and T_2 to be only modestly larger than a single layer, mimicking the relatively short coherence-to-gate-time ratios observed in contemporary NISQ hardware.

Under this normalization, T_1 values in the range of 20–50 gate units lead to γ_1 on the order of a few percent, while T_2 values around 10–20 gate units produce stronger dephasing. Accordingly, we select representative noise strengths $\gamma_1 \approx 0.02$ and $\gamma_2 \approx 0.049$, consistent with these relative coherence-time regimes.

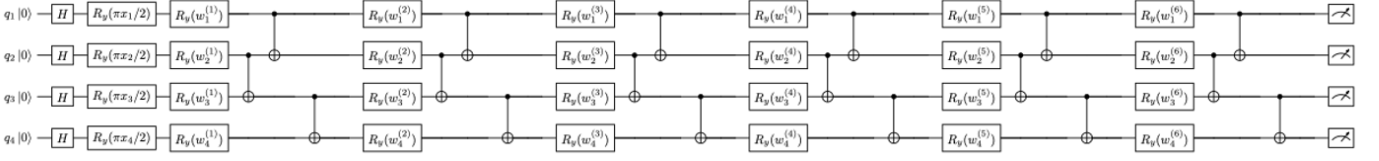


Fig. 1. Full 4-qubit variational quantum circuit used as the hybrid quantum head. The circuit begins with H gates and angle encoding $R_Y(\theta_i)$, followed by six layers of trainable R_Y rotations and ladder-style entanglement. Expectations of the Pauli- Z operator are measured on all qubits at the output.

We incorporate three noise mechanisms into the VQC, using a density-matrix simulator:

- **Amplitude damping (T₁-like).**
- **Phase damping (T₂-like).**
- **Coherent over-rotation noise.** Each intended rotation angle θ is perturbed by a zero-mean Gaussian offset,

$$\theta \mapsto \theta + \delta\theta, \quad \delta\theta \sim \mathcal{N}(0, \epsilon^2),$$

where ϵ is the standard deviation of the control miscalibration. This models systematic but randomly fluctuating pulse-shaping errors, a common source of coherent noise on real hardware.

Hybrid models under noise are trained end-to-end with the noise channels active during both forward and backward passes. This enables the variational parameters to partially adapt to the underlying noise distribution. Gradients are computed through the density-matrix simulator’s differentiation rules, ensuring stable optimization in the presence of stochastic or coherent errors.

III. EXPERIMENTS AND RESULTS

A. Training Setup

All models are implemented in PyTorch. For the classical baseline we use AdamW with weight decay and a cosine-annealing schedule. For the hybrid and ensemble models we use Adam optimizers, assigning a higher learning rate to the quantum parameters than to the surrounding classical layers. Batch sizes range from 32 to 64 depending on the model and experiment.

We train on the training split and monitor performance on the validation split, saving the checkpoint with the best validation accuracy for each model or expert. For the ensemble, each of the 5 experts is trained independently with its own bootstrap sample. Unless otherwise noted, reported test accuracies are obtained by evaluating the selected checkpoint(s) once on the held-out test set.

B. Classical vs. Hybrid Models (Noiseless)

Table I summarizes the main results on the noise-free simulator.

The single hybrid model improves accuracy by a few percentage points over the classical baseline, indicating that even a small 4-qubit VQC operating on a 4D projection of the embedding can capture useful nonlinear structure that a purely linear head does not. The 5-expert hybrid ensemble further increases test accuracy and, more importantly, reduces

TABLE I
VERIFICATION-STYLE TEST ACCURACY ON THE HELD-OUT TEST SET (340 IMAGES) WITHOUT QUANTUM NOISE.

Model	Test Accuracy	Correct / Total
ResNet-18 + FC head	90.29%	307 / 340
Hybrid single VQC head	92.94%	312 / 340
Hybrid ensemble (5 experts)	94.12%	320 / 340

the variability across random seeds and training runs. In our experiments, the ensemble typically matches or slightly exceeds the best single hybrid model while behaving more stably.

C. Noise Resilience of the Hybrid Ensemble

We next introduce quantum noise into the variational circuit and evaluate how classification accuracy changes under different noise channels. For each noise configuration, new hybrid models are trained end-to-end with the corresponding noise operators enabled during both training and inference.

Across all tested settings, several consistent trends emerge:

- **T₁ / T₂ damping produces only mild degradation.** Under amplitude and phase damping (with $\gamma_1 = 0.02$ and $\gamma_2 = 0.049$), the single-circuit hybrid model decreases slightly from the noise-free 92.94% to 92.65%, indicating that moderate relaxation and dephasing do not strongly disrupt the 4-qubit VQC.
- **Small coherent over-rotation is largely tolerable.** With an over-rotation amplitude of $\epsilon = 0.1$ combined with damping noise, the single hybrid model maintains an accuracy of 92.94%, essentially unchanged from the ideal simulator.
- **Large coherent over-rotation is strongly destructive.** Increasing the over-rotation strength to $\epsilon = 0.5$ causes the single VQC to drop sharply to 60.00%, showing that strong systematic calibration errors dominate over stochastic damping effects.
- **The Q-Vote ensemble provides substantially improved robustness.** Across all noise settings, the ensemble remains far more stable than the single VQC. It preserves 92.94% accuracy under both T₁+T₂ noise and $\epsilon = 0.1$ over-rotation, and even under the severe $\epsilon = 0.5$ case, the ensemble achieves 85.29%—a dramatic improvement over the single model’s 60.00%.

Taken together, these results show that small hybrid ensembles retain their performance advantage even when realistic quantum noise is present. However, this advantage becomes fragile when coherent control errors become too large, as strong over-rotation cannot be fully mitigated by voting alone.

IV. DISCUSSION AND FUTURE WORK

Our results illustrate both the promise and the constraints of integrating variational quantum circuits into modern vision pipelines. Practically, a VQC can be embedded as a differentiable PyTorch module with little engineering effort, enabling fully end-to-end optimization alongside classical components.

Two main insights emerge from our experiments. First, the quantum head acts as a compact low-dimensional bottleneck: projecting a 512-dimensional embedding into four quantum features still yields competitive, and sometimes improved, performance. This suggests that shallow VCQCs may be most effective as lightweight nonlinear interfaces rather than high-capacity feature extractors. Second, small hybrid ensembles provide meaningful stability benefits. Running several shallow circuits in parallel—each independently initialized—reduces variance across runs and substantially improves robustness under noise, a strategy that aligns well with NISQ hardware limitations.

At the same time, several limitations remain. Our experiments rely on simulated noise and small-scale circuits; real devices introduce additional error sources, and it is unclear how the observed trends generalize to larger datasets or deeper ansatzes. Moreover, we evaluate primarily using accuracy, whereas verification tasks typically require more detailed metrics.

These observations motivate several directions for future work: validating the same architectures on real hardware; applying explainability tools to understand the role of the quantum head; exploring noise-aware or noise-adaptive ensembles; and extending the approach to broader vision tasks.

Overall, the study provides an early view of how hybrid models behave under realistic noise and suggests that lightweight ensembles may be a practical, NISQ-compatible path toward improving stability in quantum-enhanced vision systems.

V. CONCLUSION

This work presented a systematic study of hybrid quantum-classical models for face verification, focusing specifically on how small variational circuits behave when attached to a strong convolutional backbone and subjected to realistic NISQ-style noise. Using a pretrained ResNet-18 encoder, we evaluated three readout strategies—a classical fully connected head, a single 4-qubit hybrid head, and a diverse ensemble of hybrid experts—providing a controlled comparison between classical and quantum-enhanced processing.

Our results reveal several noteworthy patterns. Even with only four qubits and a depth-six ansatz, the hybrid head consistently matched or exceeded the classical baseline, indicating that shallow VCQCs can serve as effective nonlinear bottlenecks when paired with high-quality embeddings. The ensemble further improved both accuracy and stability, reinforcing the view that classical ensembling principles remain beneficial in quantum settings and may be particularly valuable for navigating the nonconvex and noise-sensitive optimization landscapes of VCQCs.

Injecting amplitude damping, phase damping, and coherent over-rotation noise provided a task-level picture of noise resilience. Moderate T_1/T_2 damping produced only a small reduction in accuracy, while mild coherent over-rotation was effectively mitigated through noise-aware training. In contrast, strong over-rotation induced catastrophic degradation for a single VQC but was substantially buffered by the hybrid ensemble, which retained a test precision of 85.29%. These results suggest that ensembles may play a practical role in stabilizing hybrid quantum models on near-term hardware.

While preliminary in scale, this study offers a template for evaluating hybrid quantum-classical systems under realistic noise assumptions and highlights several promising directions for future work: validating these architectures on physical quantum processors, exploring quantum-friendly embedding strategies, designing noise-adaptive ensembles, and extending the analysis to multi-class recognition and other computer-vision tasks. As quantum hardware continues to improve, such application-level benchmarks will be essential for understanding where hybrid models can provide meaningful advantages in the NISQ era.

APPENDIX A VERSIONS OF ALL PYTHON MODULES USED

```
IPython == 8.18.1
PIL == 10.2.0
argparse == 1.1
copy == 3.11.14
facenet_pytorch == 2.6.0
json == 2.0.9
matplotlib == 3.6.0
numpy == 1.26.4
pennylane == 0.43.1
re == 2.2.1
sys == 3.11.14
torch == 2.2.0+cpu
torchvision == 0.17.0+cpu
tqdm == 4.66.5
Python == 3.11.14
```

APPENDIX B HARDWARE SPECIFICATIONS OF THE COMPUTING RESOURCE USED

One core of Intel i7-11800H with RTX 3070 Laptop GPU for Jacky and 8 cores of Apple M2 for Xinning

ACKNOWLEDGMENT

The authors would like to thank the instructors of ECE733 for her guidance and feedback, as well as the teaching assistants for their support during the development of this work.

REFERENCES

- [1] D. Peral-García, J. Cruz-Benito, and F. J. García-Péñalvo, “Systematic literature review: Quantum machine learning and its applications,” *Computer Science Review*, vol. 51, Art. 100619, 2024. doi: 10.1016/j.cosrev.2024.100619.

- [2] D. Peral-García, J. Cruz-Benito, and F. J. García-Péñalvo, “Comparing natural language processing and quantum natural processing approaches in text classification tasks,” *Expert Systems with Applications*, vol. 254, Art. 124427, 2024. doi: 10.1016/j.eswa.2024.124427.
- [3] J. Landman, S. Thabet, C. Dalyac, H. Mhiri, and E. Kashefi, “Classically approximating variational quantum machine learning with random Fourier features,” *arXiv preprint arXiv:2210.13200*, 2022. doi: 10.48550/arxiv.2210.13200.
- [4] E. Fontana, N. Fitzpatrick, D. M. Martín-Ramo, R. Duncan, and I. Rungger, “Evaluating the noise resilience of variational quantum algorithms,” *Physical Review A*, vol. 104, no. 2, Art. 022403, 2021. doi: 10.1103/PhysRevA.104.022403.
- [5] M. L. Olivera-Atencio, L. Lamata, and J. Casado-Pascual, “Impact of amplitude and phase damping noise on quantum reinforcement learning: challenges and opportunities,” *The European Physical Journal Special Topics*, 2025. doi: 10.1140/epjs/s11734-025-01760-3.
- [6] C. van Rossum, S. Shrapnel, and R. Gupta, “Exploiting biased noise in variational quantum models,” *arXiv preprint arXiv:2510.24050*, 2025. doi: 10.48550/arxiv.2510.24050.
- [7] J. Liu, K. H. Lim, K. L. Wood, W. Huang, C. Guo, and H.-L. Huang, “Hybrid quantum-classical convolutional neural networks,” *Science China Physics, Mechanics & Astronomy*, vol. 64, no. 9, Art. 290311, 2021. doi: 10.1007/s11433-021-1734-3.
- [8] E. H. Houssein, Z. Abohashima, M. Elhoseny, and W. M. Mohamed, “Hybrid quantum-classical convolutional neural network model for COVID-19 prediction using chest X-ray images,” *Journal of Computational Design and Engineering*, vol. 9, no. 2, pp. 343–363, 2022. doi: 10.1093/jcde/qwac003.
- [9] G. Chen, Q. Chen, S. Long, W. Zhu, Z. Yuan, and Y. Wu, “Quantum convolutional neural network for image classification,” *Pattern Analysis and Applications*, vol. 26, no. 2, pp. 655–667, 2023. doi: 10.1007/s10044-022-01113-z.
- [10] Y. Zhu, A. Bouridane, M. E. Celebi, D. Konar, P. Angelov, Q. Ni, and R. Jiang, “Quantum face recognition with multigate quantum convolutional neural network,” *IEEE Transactions on Artificial Intelligence*, vol. 5, no. 12, pp. 6330–6341, 2024. doi: 10.1109/TAI.2024.3419077.
- [11] A. Mari, T. R. Bromley, J. Izaac, M. Schuld, and N. Killoran, “Transfer learning in hybrid classical–quantum neural networks,” *Quantum*, vol. 4, Art. 340, 2020. doi: 10.22331/q-2020-10-09-340.
- [12] M. A. Nielsen and I. L. Chuang, *Quantum Computation and Quantum Information*, 10th ed. Cambridge, U.K.: Cambridge University Press, 2010.
- [13] A. Callison and N. Chancellor, “Hybrid quantum-classical algorithms in the noisy intermediate-scale quantum era and beyond,” *Physical Review A*, vol. 106, no. 1, 010101, 2022. doi: 10.1103/PhysRevA.106.010101.
- [14] D. Ranga, S. Prajapat, Z. Akhtar, P. Kumar, and A. V. Vasilakos, “Hybrid Quantum–Classical Neural Networks for Efficient MNIST Binary Image Classification,” *Mathematics (Basel)*, vol. 12, no. 23, 3684, 2024. doi: 10.3390/math12233684.
- [15] Y. Mei, “ResNet18 facial feature extraction algorithm improved based on hybrid domain attention mechanism,” *PloS One*, vol. 20, no. 3, e0319921, 2025. doi: 10.1371/journal.pone.0319921.